Combustion and Flame 157 (2010) 667–675

Contents lists available at ScienceDirect

Combustion and Flame

journal homepage: www.elsevier.com/locate/combustflame

Laminar burning velocities and Markstein lengths of premixed methane/air flames near the lean flammability limit in microgravity

Shuang-Feng Wang [a,*], Hai Zhang [b], Jozef Jarosinski [c], Andrzej Gorczakowski [c], Jerzy Podfilipski [c]

[a] National Microgravity Laboratory, Institute of Mechanics, Chinese Academy of Sciences, Beijing 100190, China
[b] Department of Thermal Engineering, Tsinghua University, Beijing 100084, China
[c] Department of Heat Technology and Refrigeration, Technical University of Lodz, Stefanowskiego 1/15, 90-924 Lodz, Poland

ARTICLE INFO

Article history:
Received 12 March 2009
Received in revised form 16 October 2009
Accepted 11 January 2010
Available online 3 February 2010

Keywords:
Laminar burning velocity
Markstein length
Near-limit flames
Flame stretch
Microgravity

ABSTRACT

Effects of flame stretch on the laminar burning velocities of near-limit fuel-lean methane/air flames have been studied experimentally using a microgravity environment to minimize the complications of buoyancy. Outwardly propagating spherical flames were employed to assess the sensitivities of the laminar burning velocity to flame stretch, represented by Markstein lengths, and the fundamental laminar burning velocities of unstretched flames. Resulting data were reported for methane/air mixtures at ambient temperature and pressure, over the specific range of equivalence ratio that extended from 0.512 (the microgravity flammability limit found in the combustion chamber) to 0.601. Present measurements of unstretched laminar burning velocities were in good agreement with the unique existing microgravity data set at all measured equivalence ratios. Most of previous 1-g experiments using a variety of experimental techniques, however, appeared to give significantly higher burning velocities than the microgravity results. Furthermore, the burning velocities predicted by three chemical reaction mechanisms, which have been tuned primarily under off-limit conditions, were also considerably higher than the present experimental data. Additional results of the present investigation were derived for the overall activation energy and corresponding Zeldovich numbers, and the variation of the global flame Lewis numbers with equivalence ratio. The implications of these results were discussed.

1. Introduction

The laminar burning velocity is one of the fundamental properties of a reacting premixed mixture, and its reliable data are constantly needed for combustion applications. Since the late 1970s, there have evolved significant advances to understand the effects of flame stretch on the laminar burning velocity. Failure to account for the stretch effects may well explain the large spread in reported burning velocity values from earlier investigations [1,2]. So far, several techniques for measuring the one-dimensional laminar burning velocity have been used, and for a wide range of temperature, pressure, and fuel rather accurate measurements have been obtained by employing flat or curved flames in stagnation flow (e.g., [3–7]), propagating spherical flames in combustion vessel (e.g., [8–12]), or flat flames stabilized on burner [13,14]. With all those measurement techniques proper care could be taken to remove the effect of flame stretch either during experimentation or through further data processing.

For the laminar burning velocity of methane/air mixtures, a substantial improvement in consistency among the measurements was achieved in recent years due to the recognition of the influence of flame stretch and the resulting corrections for it [10,14]. For example, for the stoichiometric CH_4/air flame, recent experiments converge toward a value around 36 cm/s, and the differences between the results of different measurement techniques do not vary by more than roughly 1 cm/s [14]. However, at lower and higher equivalence ratios there is still noticeable variation among burning velocity data from various sources. The situation is even less satisfactory for very lean and very rich flames since the scatter tends to widen as the limits of flammability are approached. Particularly, few measurements have been performed for the weakly-burning near-limit mixtures.

Part of the difficulty stems from the fact that, when the flames are weaker, they become more sensitive to experimental errors. However, a major complicating factor is the influence of gravitational effects. For weakly-burning near-limit mixtures, flames at earth gravity (i.e., 1-g) become greatly affected by buoyant distortion because the gas speed driven by natural convection is of the same order as the burning velocity. The problem of this type has been consistently observed during previous experiments and was stressed in reviews of microgravity combustion [15–17]. The gen-

* Corresponding author. Address: National Microgravity Laboratory, Institute of Mechanics, Chinese Academy of Sciences, Beijing 100190, China. Fax: +86 10 8254 4096.
E-mail address: sfwang@imech.ac.cn (S.-F. Wang).

0010-2180/$ - see front matter © 2010 The Combustion Institute. Published by Elsevier Inc. All rights reserved.
doi:10.1016/j.combustflame.2010.01.006

Nomenclature

E	activation energy
I	correction factor, as defined
Ka	Karlovitz number
L, L_b, L_r	Markstein lengths, as defined
Le	Lewis number
Ma	Markstein number
n	mole ratio
R	universal gas constant
r	radius
r_{sch}	schlieren flame front radius
r_u	cold flame front radius
S	stretched flame speed
S_0	unstretched flame speed
t	time
T_{ad}	adiabatic flame temperature
T_b	burned gas temperature
T_r	temperature at radius r
T_u	unburned mixture temperature
u_L	stretched laminar burning velocity
u_g	gas velocity induced by flame expansion
u_{L0}	unstretched laminar burning velocity
$u_{L0,\,lim}$	u_{L0} at flammability limit
V	volume encircled by flame front
Ze	Zeldovich number
α	total stretch rate
α_c	stretch rate due to flame curvature
α_s	stretch rate due to strain
ϕ	fuel-equivalence ratio
ρ_b	density of burned gas
$\overline{\rho_b}$	mean density of gas within flame front r_u
ρ_u	density of unburned mixture
δ	flame thickness
δ_0	characteristic thickness of one-dimensional flame
δ_L	characteristic laminar flame thickness given by $\delta_L = \nu/u_{L0}$
ν	kinematic viscosity of unburned mixture

eral cognition is that conducting experiments under microgravity conditions is essential for eliminating the complications of buoyancy and thus enabling reliable measurements of near-limit flame properties. In fact, the behaviors of CH_4/air flames near lean limit have been examined by several experimental investigations in microgravity [18–23]. Most of those studies were concerned with flame extinction phenomena and flammability limits, while the burning velocities of near-limit flames have not received much attention. One exception is the study of Ronney and Wachman [20], in which lean limit compositions and near-limit values of the burning velocity were determined for CH_4/air mixtures utilizing outwardly propagating spherical flames in a cylindrical vessel; those authors have also inferred the near-limit burning velocities for the microgravity experiments of Strehlow and Reuss [18], in which corresponding flame propagation speeds were measured for lean CH_4/air mixtures using a standard flammability tube; nevertheless, the effects of flame stretch were not considered, while the reported burning velocities were for stretched flames.

In view of the above considerations, the main objective of the present study is to determine the laminar burning velocities and the sensitivities of the flame response to stretch for near-limit lean CH_4/air flames. Using a microgravity environment, weakly burning CH_4/air flames having fuel-equivalence ratios in a range of 0.512–0.601 are studied at ambient initial temperature and pressure. Outwardly propagating spherical flames are employed to measure flame speeds, from which corresponding stretched and unstretched laminar burning velocities are derived. Associated Markstein lengths are obtained to express the effects of flame stretch on the burning velocities. Also extracted are the activation energy and Zeldovich numbers representing the sensitivity of chemical reactions to flame temperature, and the global flame Lewis numbers. Measured unstretched laminar burning velocities are compared with those from a numerical prediction utilizing the one-dimensional flame model with a full kinetic mechanism. Where data are available, present results are compared with those of other studies.

2. Experimental

2.1. Apparatus

The experimental package consisted of a closed combustion chamber, spark generator, high-speed schlieren system, video camera, and pressure measurement system. The package was mounted in a steel framework and used for all 1-g and microgravity tests.

The 80-mm-inner-length, cubic, stainless steel combustion chamber could be operated over a pressure range extending from vacuum to a maximum of 15 bar. Optical access was provided by two 80 mm length square quartz windows mounted opposite one another. Reactant mixtures were prepared within a sealed separated vessel by blending methane and air at appropriate flow rates controlled with mass flow controllers (Alicat Scientific, type MC). Accuracy of the mixture composition was estimated to be ±0.02% in the listed values in Table 1. The combustion chamber was exhausted prior to filling it with the prepared reactant mixture to reach a pressure slightly higher than the ambient pressure (i.e., 1 atm). The exhausting and filling procedure was repeated for five times to ensure that the chamber would be indeed filled with the specified mixture. After the mixture filling operation was complete, a vent valve on the chamber was opened manually for several seconds to balance pressure inside the chamber and ambient pressure. Methane/air mixtures were studied at a constant temperature of 298 ± 2 K for fuel-equivalence ratios between 0.512 and 0.601 (corresponding fuel concentrations between 5.09% and 5.92%). The lowest equivalence ratio of 0.512 is the lean flammability limit of methane in air that was found from the present microgravity tests.

The mixture was ignited by a spark at the center of the chamber using two electrodes extending from the bottom and one side wall. The flame propagation was observed with the high-speed schlieren photography system. Flame pictures were recorded using a high-speed digital video camera (Redlake MotionScope M1) at 500 frames per second. Additionally, the pressure history in the chamber, which could be correlated with the flame propagation records, was measured by using a membrane type strain-gauge transducer located at the bottom of the chamber.

Microgravity experiments were performed in the free-fall facility at the combustion laboratory of the Technical University of Lodz, Poland. In this facility (see [24] and [25] for a detailed description), the experimental package experiences 1.2 s of 10^{-3}–10^{-2} g reduced gravity. Immediately prior to the release of the package, the high-speed video camera was triggered and a computer began to record the signal from the pressure transducer. As the package was released, a timer was triggered. After a short delay to allow oscillations from the release to decay, a timer pulse trig-

Table 1
Summary of experimental results.

ϕ	Methane concentration in air (%)	ρ_u/ρ_b	v (cm^2/s)	u_{L0} (cm/s)	L_b (cm)	L (cm)	L_r (cm)	Ze	Le
0.512	5.09	5.040	0.1553	1.2	−0.62	−0.22	−0.097	28.6	0.910
0.52	5.17	5.095	0.1553	1.5	−0.57	−0.21	−0.089	28.4	0.910
0.529	5.25	5.149	0.1553	1.7	−0.55	−0.19	−0.086	28.1	0.909
0.536	5.32	5.196	0.1553	2.0	−0.47	−0.17	−0.072	27.9	0.912
0.545	5.40	5.249	0.1553	2.5	−0.43	−0.16	−0.064	27.7	0.914
0.564	5.58	5.369	0.1553	3.7	−0.31	−0.12	−0.045	27.2	0.923
0.585	5.77	5.494	0.1554	5.4	−0.25	−0.10	−0.033	26.8	0.926
0.601	5.92	5.592	0.1554	6.7	−0.18	−0.08	−0.021	26.4	0.933

gered the spark generator to ignite the mixture. For each reactant mixture, 3–5 microgravity tests were carried out.

2.2. Data processing

The flame speed, S, was derived from the measurements of flame front radius against time as

$$S = \frac{dr_u}{dt} \tag{1}$$

where r_u is the radius of the cold flame front. Bradley et al. [26], in their computational study of spherical flame propagation, defined r_u as the isotherm that is 5 K above the temperature of the reactants, and showed r_u to be related to the flame front radius observed by schlieren photography, r_{sch}, by

$$r_u = r_{sch} + 1.95\delta_L\left(\frac{\rho_u}{\rho_b}\right)^{0.5} \tag{2}$$

where ρ_u is the density of the unburned mixture, ρ_b that of the burned gas at the adiabatic flame temperature, and δ_L is a characteristic laminar flame thickness calculated by $\delta_L = v/u_{L0}$, in which v is the kinematic viscosity of the unburned mixture and u_{L0} the laminar burning velocity for an unstretched planar flame. Because u_{L0} cannot be determined before r_u is known (and vice versa), it was first estimated using r_{sch} and then Eq. (2) was adopted to give r_u.

The schlieren images were analyzed to determine r_{sch}. Image analyses involved a binarization process to mark the flame front and then taking the coordinates of the flame. Once the flame coordinates were obtained, the volume encircled by the flame front, V, could be calculated by assuming that the flame was a rotating face about the vertical axis. The value of r_{sch} was calculated from V based on the equivalent volume. During the measurements of r_{sch}, there was no significant rise in chamber pressure; in all cases the pressure increment was less than 80 mbar. The lower radius limit of processing was between 11 and 15 mm since the flame propagation seemed independent of the spark ignition process beyond this limit. For an outwardly propagating spherical flame, the total stretch rate at the cold front of radius r_u is given by

$$\alpha = \frac{2S}{r_u} \tag{3}$$

It consists of the stretch due to both flame curvature, $\alpha_c = 2u_L/r_u$, and aerodynamic strain, $\alpha_s = 2u_g/r_u$, where u_L is the stretched laminar burning velocity, and $u_g = S - u_L$ the gas velocity induced by the flame expansion at r_u. According to Bradley et al. [26] and Clavin [27], a linear relationship between S and α exists, and a burned gas Markstein length, L_b, can be defined in

$$S = S_0 - L_b\alpha \tag{4}$$

Here S_0 is the unstretched flame speed, and is obtained by extrapolating S to $\alpha = 0$. The gradient of the best straight line fit to the plot of S against α gives L_b. By definition, u_{L0} is related with S_0 by

$$u_{L0} = S_0\frac{\rho_b}{\rho_u} \tag{5}$$

According to the previous study [26], the relationship between u_L and S for spherical flame propagation is expressed as

$$u_L = \frac{\overline{\rho_b}}{\rho_u}S + \frac{r_u}{3\rho_u}\frac{d\overline{\rho_b}}{dt} \tag{6}$$

where $\overline{\rho_b}$ is the mean density of the gas within the flame front r_u. Clearly, $\overline{\rho_b}$, instead of ρ_b, appears in Eq. (6) as a consequence of the fact that any real flame has a finite thickness, δ, and the difference between $\overline{\rho_b}$ and ρ_b may be prominent for near-limit flames as a result of their great thickness. The radial temperature distribution in a spherical flame kernel is shown schematically in Fig. 1. This assumes that the burned gas within $(r_u - \delta)$ is at a constant temperature T_b, and the temperature profile through the flame decreases from T_b to the unburned mixture temperature, T_u. For the temperature distribution of Fig. 1, it can be shown [1] that

$$\frac{\overline{\rho_b}}{\rho_u} = \frac{nT_u}{T_b}I = \frac{\rho_b}{\rho_u}I \tag{7}$$

with

$$I = \frac{1}{r_u^3}\left[(r_u - \delta)^3 + 3T_b\int_{r_u-\delta}^{r_u}\frac{r^2\,dr}{T_r}\right] \tag{8}$$

Here n is the ratio of total moles per unit mass in the unburned gas to total moles per unit mass in the burned gas, and I could be regarded as a correction factor that makes allowance for the temperature variation through the flame.

Values of I were evaluated from Eq. (8) on the assumptions that the shape of the temperature profile through the flame is linear, that T_b is equal to the adiabatic flame temperature T_{ad}, and that flame thicknesses are as determined by Andrews and Bradley [1]. Shown in Fig. 2 are the variations of the derived values of I with flame radius for three near-limit CH_4/air flames. The leaner the mixture is (so that the thicker the flame becomes) and/or the smaller the flame radius is, the greater will I becomes, implying the increasing importance of the allowance for flame thickness in the determination of u_L. Even at a rather large radius of $r_u = 70$ mm for $\phi = 0.585$, however, I still has a value of 1.13, notably greater than unity.

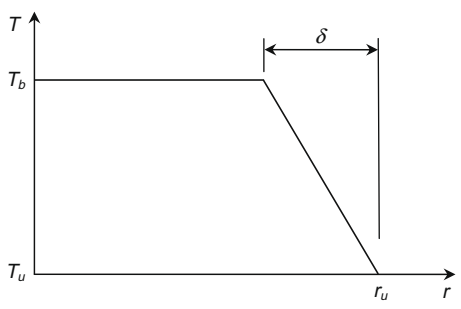

Fig. 1. Temperature distribution in a spherical flame kernel.

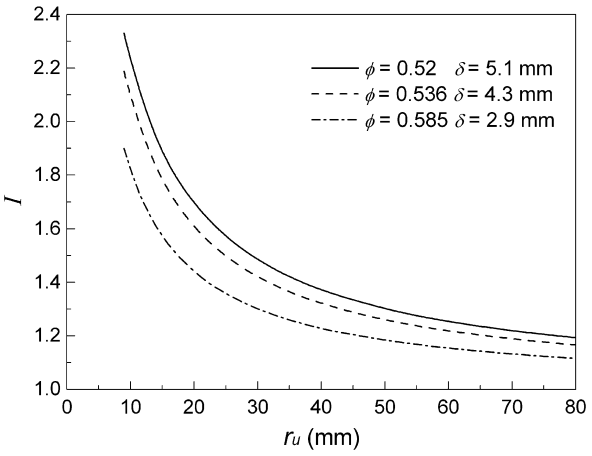

Fig. 2. Variation of flame thickness factor, I, with flame radius for near-limit CH_4/air flames at three different equivalence ratios.

The relationship between u_L and α is based on an early proposal of Markstein [28], after later generalization by Clavin [27], written as

$$u_L = u_{L0} - L\alpha \tag{9}$$

Here L is the Markstein length, a measure of the sensitivity of premixed flames to stretch. The unstretched laminar burning velocity, u_{L0}, could be obtained by extrapolating u_L to zero stretch, while L was derived as the gradient of the best straight line fit to the measured u_L against α data. Although some methodologies were adopted in the literature (e.g., [8,9]) to characterize the flame response to stretch in terms of a dimensionless stretch rate (called the Karlovitz number, Ka) and a dimensionless Markstein length (the Markstein number, Ma), it is more direct to simply express this response in terms of the dimensional quantities as Eq. (9) does. The advantage of using L and α over Ma and Ka is that they are well defined while the magnitudes of Ma and Ka can be quite uncertain [29].

3. Computational approach

The burning velocity of a steady, one-dimensional, planar, laminar premixed flame was computed using the well-established Sandia PREMIX code [30]. The chemical reaction mechanism used was GRI-Mech 3.0 [31], which describes the methane oxidation chemistry in terms of 325 elementary reactions of 53 species.

The values of ρ_b, T_{ad} and n were found from the calculated properties of the equilibrated products, based on the thermodynamic data base of GRI-Mech 3.0. Also, from this data base, specific heats at constant pressure were obtained for pure gases in the reactant mixture. The mixture-averaged specific heat, c_p, was then calculated with the mass fraction of pure gases. Pure gas viscosities and thermal conductivities were found from the transport data base of GRI-Mech 3.0. The mixture-averaged viscosity, ν, was calculated using the semi-empirical formula proposed by Wilke [32] and modified by Bird et al. [33]. For the mixture thermal conductivity, λ, the combination averaging formula of Mathur et al. [34] was adopted. The thermal diffusivity of the mixture was then calculated as $\lambda/(c_p\rho_u)$. The mass diffusivity of the deficient reactant, methane, relative to the abundant species, nitrogen, was obtained as a representative mass diffusivity of the mixture. The radiative heat loss from the species of CO_2, H_2O, CO and CH_4 was considered by using the optically thin assumption.

4. Results and discussion

The flammability limit definition proposed by Ronney and Wachman [20] has been employed in the current study. Namely, the microgravity flammability limit in a closed vessel is the limiting mixture composition for quasi-steady flame propagation throughout the vessel at microgravity. Such a limit is well defined and can be readily determined because of the abrupt change in the flame behavior found at it. In the present microgravity observations the lean flammability limit was 5.09% CH_4 in air (ϕ = 0.512), quite close to Ronney and Wachman's experimental finding of 5.07% CH_4. Certainly, this may differ from the fundamental flammability limit, which was defined for the propagation of the one-dimensional, planar, steady, laminar flame configuration [35], while the present value is generally consistent with reported data in the literature.

4.1. Influence of gravity on flame propagation

For the near-limit mixtures considered herein, buoyancy at 1-g had notable influence on flame propagation. The buoyancy effects increased with decreasing methane concentration in a mixture. For mixture concentrations above 5.58% CH_4 (ϕ = 0.564), a flame front at 1-g reached the top of the chamber before reaching the bottom. For still leaner, slower burning mixtures, at 1-g a flame could not propagate downward against the gas rise flow induced by buoyant force. The flame was seen to move upward to form a classical mushroom shape, and then spread laterally and downward after reaching the top of the chamber. For leanest mixtures (ϕ = 0.529, 0.52, and 0.512), the upward propagating flame could not even spread downward after reaching the chamber top, so approximately only a half of the mixture volume would be consumed in the combustion chamber. The flame propagation at microgravity was completely different from that at 1-g. In all cases, the flame front remained smooth and nearly spherically symmetrical, although it was observed to flatten somewhat near the electrodes, probably induced by conductive heat loss [20]. The effects of gravity were manifested also by the pressure histories in the chamber. In Fig. 3, the maximum pressures, P_{max}, obtained at 1-g and microgravity, are shown as a function of ϕ, together with the calculated theoretical values. The pressure rise at microgravity is invariably larger than that at 1-g, and the difference decreases as ϕ increases.

4.2. Influence of stretch on flame speed and burning velocity

A selection of measured flame speeds, S, is plotted against flame radius, r_u, in Fig. 4 for four equivalence ratios. At small flame radii the speeds are high. As the flames expand, their speeds fall and the rates of flame deceleration also decrease with the increase of r_u.

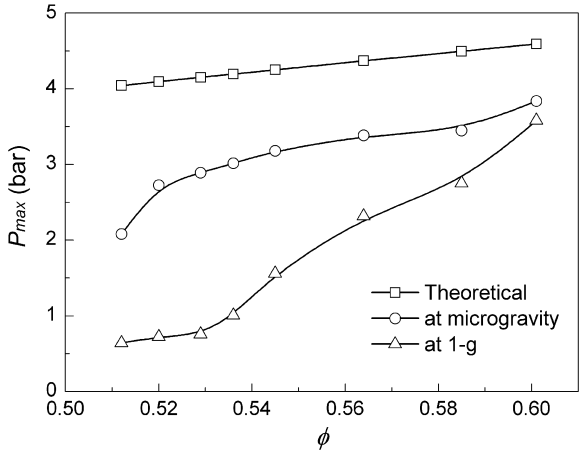

Fig. 3. Maximum pressures obtained in 1-g and microgravity experiments together with theoretical values as a function of equivalence ratio.

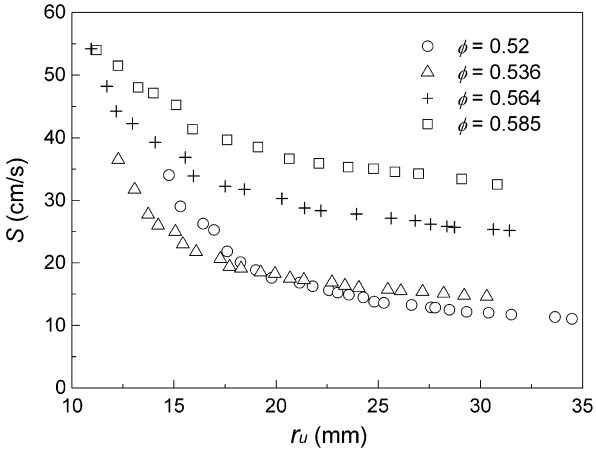

Fig. 4. Variations of flame speeds with flame radius for different equivalence ratios.

Shown in Fig. 5 are the variations of S with stretch rate, α, for the same mixtures illustrated in Fig. 4. Values of α are given by Eq. (3) and are highest at small radii. For all mixtures, S decreases with the decreasing α as the flame propagates outwardly, indicative of a negative burned gas Markstein length, L_b. However, the effect of stretch on the flame speed changes with ϕ, and the flame becomes more sensitive to stretch when ϕ decreases. The variations of S with α, shown in Fig. 5, are reasonably linear over the measured range of flame radius. Consequently, a linear extrapolation of S to zero stretch gives the unstretched flame speed, S_0, and the gradient yields a single value of L_b.

The effect of flame stretch on u_L is shown in Fig. 6. Values of u_L were obtained from Eq. (6) with the method described earlier. Again, increasing flame stretch has a favorable effect on the increase of u_L, resulting in a negative Markstein length L. Following Strehlow and Savage [36], u_L was frequently related to S by a quasi-steady expression $u_L = (\rho_b/\rho_u)S$. The expression assumes zero flame thickness, and, as demonstrated in Section 2, can bring significant error. Andrews and Bradley [1,37] recommended a correction to this comparatively simple equation to account for finite flame thickness, in which u_L was equated to S divided by the ratio of the unburned mixture density to the mean density of the gas within the flame front, i.e., $u_L = (\overline{\rho_b}/\rho_u)S$. Actually, as an expression for u_L, it neglects the $d\overline{\rho_b}/dt$ term on the right-hand of Eq. (6). Values of u_L determined in this way are also plotted in Fig. 6. They are consistently higher than the values from Eq. (6), as is reasonable to expect since the $d\overline{\rho_b}/dt$ term in Eq. (6) is always negative for spherically expanding flames. It is worth mentioning that, for a given mixture, both u_L data in Fig. 6 yield almost the same value of u_{L0} at $\alpha = 0$ if they are linearly extrapolated.

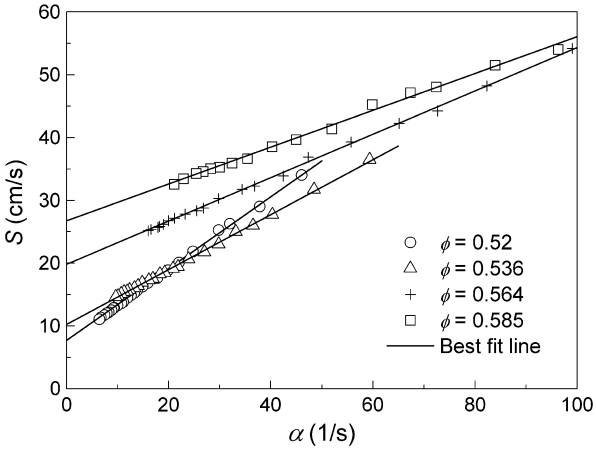

Fig. 5. Variations of flame speeds with flame stretch rate for different equivalence ratios.

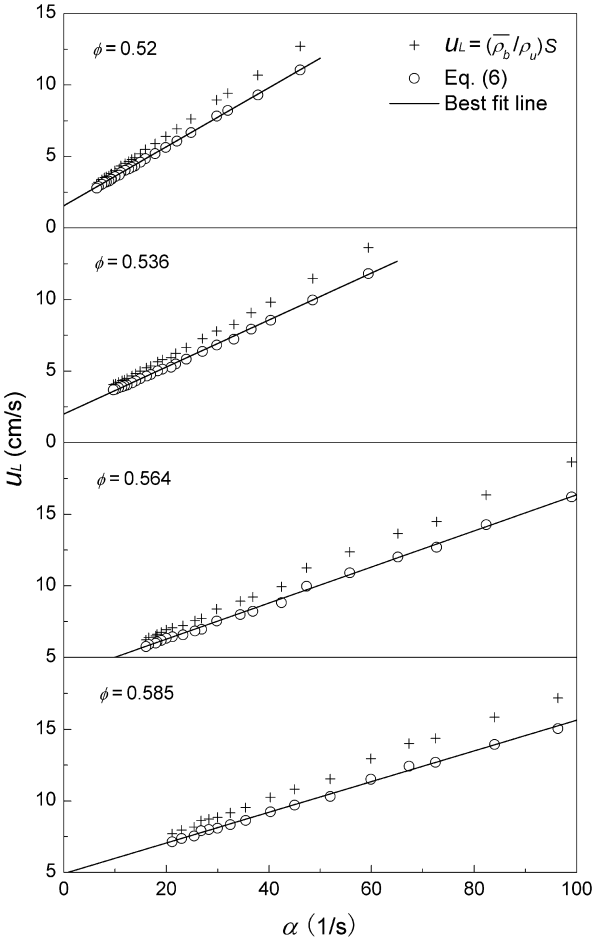

Fig. 6. Variations of laminar burning velocities with flame stretch rate for different equivalence ratios.

The results illustrated in Figs. 4–6 indicate that the effects of flame stretch on S and u_L are substantial. For example, S and u_L decrease by factors of 3.1 and 3.9, respectively, for the present range of flame radius as the flame expands at $\phi = 0.52$. Even at $\phi = 0.585$ where the flame is somewhat less sensitive to stretch, S and u_L change by factors of 1.6 and 2.1, respectively. One more point to note is that because the gas velocity induced by flame expansion, u_g (=$S - u_L$), is typically 2–4 times the magnitude of u_L, the stretch due to aerodynamic strain prevails over that due to flame curvature under the investigated conditions.

4.3. Unstretched laminar burning velocities

In the present study two independent methods have been utilized to determine the values of u_{L0}. One set of values was deduced from S_0 using Eq. (5), and another from u_L using Eq. (9). The resulting two sets of u_{L0} are plotted as a function of ϕ in Fig. 7. They are in good agreement with each other, demonstrating the consistency and hence meaningfulness of the employed approach to data processing. Values of u_{L0} derived from u_L are summarized in Table 1 and will be used in further analyses.

The present results of u_{L0} are compared in Fig. 8 with experimental data of other sources and computed predictions of both the present work and previous studies. Data for laminar burning

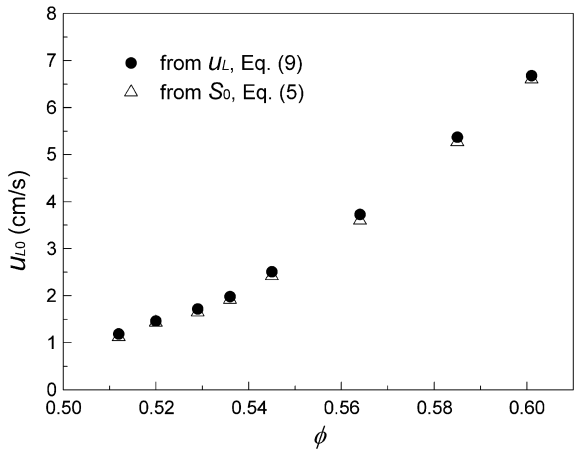

Fig. 7. Unstretched laminar burning velocities measured in present study as a function of equivalence ratio.

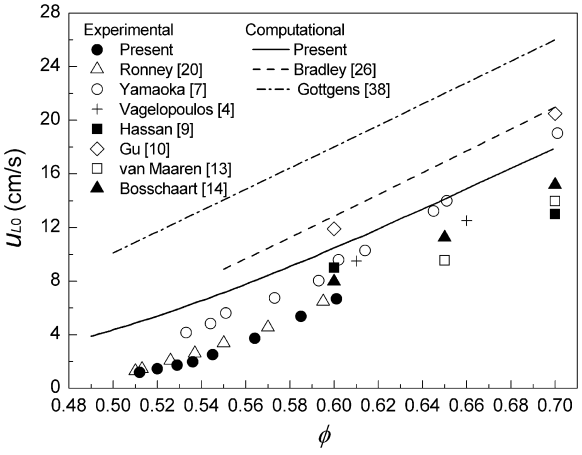

Fig. 8. Measured and computed unstretched laminar burning velocities by various workers as a function of equivalence ratio.

velocities of CH_4/air flames near the flammability limit are sparse. However, more experiments are available for $\phi \geqslant 0.6$ mixtures. Data sources have been therefore quoted up to $\phi \approx 0.7$ to obtain an extended comparison.

Outwardly propagating spherical flames have been used by Ronney and Wachman [20], Hassan et al. [9] and Gu et al. [10]. The first case is special because a microgravity environment was utilized and reliable burning velocity data could be obtained for slow-burning mixtures until the flammability limit was reached. They did not report values of u_{L0}, but rather values of u_L, which were evaluated from the flame speed at a flame radius of 70 mm using the expression $u_L = (\rho_b/\rho_u)S$. For the purpose of comparing, the data shown in Fig. 8 have been corrected to u_{L0} by using Eqs. (6) and (9) to account for nonzero flame thickness and flame stretch effects, respectively. The correction varied from −0.2 cm/s to −0.5 cm/s, with the magnitude increasing with ϕ generally. In the other two cases, they determined u_{L0} from measured S or u_L by extrapolating to zero stretch. Vagelopoulos et al. [4] used the counterflow twin-flame technique for the determination of u_{L0}. Particularly, they provided further insight into the accuracy of the linear extrapolation practice. Their redetermined values of u_{L0} were found to be lower than previous results obtained using the same technique. Yamaoka and Tsuji [7] measured u_L by using another type of counterflow flames, and reported data for low stretch conditions. By utilizing Eq. (9) to correct u_L for flame stretch, corresponding values of u_{L0} have been evaluated and indicated in Fig. 8. The correction varied from −1.5 cm/s to 2.2 cm/s, depending on α and ϕ. van Maaren et al. [13] and Bosschaart and de Goey [14] obtained u_{L0} data using the so-called heat flux method. In this method it was possible to create nearly stretchless flat adiabatic flames with a perforated plate burner.

Compared with earlier measurements of the burning velocity [1,2], Fig. 8 clearly demonstrates an improvement in consistency of the experimental data. Particularly, there is good agreement between values obtained by the present experiments and Ronney and Wachman [20] at all measured equivalence ratios. The trend expected from these two microgravity data sets seems to be followed by the data of van Maaren et al. [13] for $\phi > 0.6$. However, bearing the fact in mind that the near-limit burning velocities are rather low, the deviations of the results in Fig. 8 are still relatively large. An observed tendency is that most of previous 1-g experiments resulted in laminar burning velocities that are significantly higher than the present and previous microgravity results. Because the near-limit flames are sensitive to errors, further experiments are required to examine the true values of u_{L0}.

Previous predictions shown in Fig. 8 include the computations by Bradley et al. [26] and Göttgens et al. [38]. In the former case, numerical simulations of outwardly propagating spherical flames were performed to deduce u_{L0}. The reduced kinetic mechanism of Mauss and Peters [39] was employed for a range of equivalence ratio. The computation by Göttgens et al. was for one-dimensional flames using a detailed mechanism of 82 reactions. Bradley et al. predicted burning velocities much higher than the present experimental values. Compared with other data sources, their computation shows a similar, but somewhat slighter overprediction, although the data of Gu et al. [10] appear to agree with it. The computed results of Göttgens et al. are even higher than those of Bradley et al., showing an obvious overprediction. The present numerical predictions using GRI-Mech 3.0 mechanism also give higher values than the present experiments at all equivalence ratios, although they are systematically lower than the predictions of Bradley et al. This discrepancy is expected to be caused by the chemical mechanism, which was tuned mainly with laminar burning velocities of methane under off-limit conditions.

Present measurements show that u_{L0} at the flammability limit, here denoted by $u_{L0,\,lim}$, is equal to 1.2 cm/s. The microgravity experiments by Ronney and Wachman [20] reached a similar limit value for CH_4/air flame, which takes $u_{L0,\,lim} \approx 1.3$ cm/s after the minor correction described above. Previous computations [40,41] have shown that there is no purely chemical flammability limit for unstretched planar flame without heat losses and that u_{L0} will decrease asymptotically to zero as the dilution increases. Taking radiative heat loss into account, the computation of Lakshmisha et al. [42] showed that heat losses can play a significant role in flame extinction and gave a limiting flame speed of 2 cm/s. A theoretical estimation of $u_{L0,\,lim}$ for radiative heat loss was given by Williams [35]. It seemed to predict $u_{L0,\,lim} \approx 2.3$ cm/s for lean-limit hydrocarbon/air mixtures [17]. It is noted that the present microgravity result is consistent with previous studies, although there is no good agreement on the true value of $u_{L0,\,lim}$ to date.

4.4. Markstein lengths

According to Bradley et al. [11,26], there are two possible definitions of stretched burning velocity, each legitimate and pertinent in practical contexts. The first already derived, u_L, is based on the rate of disappearance of unburned mixture, the second, u_{Lr}, on the rate of appearance of burned products. The two burning velocities differ as a consequence of the finite flame thickness. As the flame radius tends to infinity, both u_L and u_{Lr} tend towards u_{L0}. Bradley et al. [26] showed that u_{Lr} and u_L are related by

$$u_{Lr} = \frac{\rho_b}{\rho_u - \rho_b}(S - u_L) \tag{10}$$

From Eqs. (4), (5), (9), and (10),

$$u_{Lr} = u_{L0} - L_r\alpha \tag{11}$$

with

$$L_r = \frac{1}{\rho_u/\rho_b - 1}(L_b - L) \tag{12}$$

where L_r is the Markstein length that expresses the influence of flame stretch on u_{Lr}. Values of L_r could therefore been derived from L_b and L, which are defined in Eqs. (4) and (9), respectively.

The three Markstein lengths, L_b, L, and L_r, are presented against ϕ in Fig. 9 and Table 1. All attain negative values and appear to vary in a similar way with ϕ over the entire range of measured conditions. The absolute values of Markstein lengths decrease with ϕ, indicating reduced stretch effect on the flame in richer mixtures. Furthermore, the variations of Markstein lengths with ϕ can be represented by straight fit lines, as shown in Fig. 9. The neutral condition, where flame properties are independent of stretch and so that Markstein length equates zero, can thus be obtained by extrapolating Markstein length to zero. From L_b, L, and L_r, this extrapolation yielded neutral conditions at $\phi_{neutral} = 0.63$, 0.65, and 0.62, respectively. They are in accord with the experimental observations of Aung et al. [8] and Hassan et al. [9]. Aung et al. suggested a linear correlation for the Markstein number as a function of ϕ and obtained $\phi_{neutral} = 0.68$. From the experiments of Hassan et al., it can be inferred that $\phi_{neutral} = 0.6$–0.7.

4.5. Zeldovich number and Lewis number

Knowing $u_{L0}[\phi(T_b)]$, the overall activation energy E for the unstretched planar flame propagation can be determined. Peters and Williams [43] have derived an asymptotic structure of methane flames that introduced an inner layer with a characteristic temperature T_0. Chemical reactions take place at temperatures around and above T_0 only. Therefore the inner layer temperature could be interpreted as the critical temperature at which chemistry is turned on [38]. Provided that T_0 is primarily a function of pressure [38,43], the dependence of the laminar burning flux, $\rho_u u_{L0}$, on the flame temperature can be expressed as [43]

$$\frac{E}{R} = -\frac{d2[\ln(\rho_u u_{L0})]}{d(1/T_b)} \tag{13}$$

where R is the universal gas constant, and E/R the activation temperature. Such that the value of E/R can be derived from the linear plot of $2\ln(\rho_u u_{L0})$ against $1/T_b$ at a given pressure. Assuming E/R does not change much in the limited range of $\phi = 0.512$–0.601, the gradient of the linear fit line yields E/R. The resulting value, together with the computed prediction of Göttgens et al. [38] and the experimental result of Gu et al. [10] at a pressure of 1 bar, are tabulated in Table 2. It is seen that although the pressures are almost the same, the present experiments give E/R much higher than previous results, and Göttgens et al. predicted a considerably higher value than the experimental result of Gu et al. An apparent explanation of this discrepancy is that E depends strongly also upon ϕ, and therefore the reported values in Table 2 should be treated as averaged ones for the investigated range of ϕ. The present value of E/R is expected more pertinent to near-limit CH_4/air flames since the measured range of ϕ is narrow.

From the value of E/R, a dimensionless form of E, designated as the Zeldovich number, can be calculated as [27]

$$Ze = \frac{E}{RT_b^2}(T_b - T_u) \tag{14}$$

It indicates the sensitivity of chemical reactions to flame temperature variations, and the inverse of it represents a dimensionless thickness of the reaction zone [29,44]. Values of Ze determined from the present E/R are shown for different equivalence ratios in Fig. 10. As ϕ increases in the measured range Ze monotonically decreases.

Conventionally estimated as the ratio of the thermal diffusivity to a representative mass diffusivity of the mixture, Lewis number, Le, is a global flame property in nature and as such should be extracted from the flame response to stretch [29,45,46]. Recognizing this concern, Sun et al. [45,46] have proposed systematic approaches through which a global, flame Lewis number could be extracted by comparing the theoretical expression for the stretched flame response with the corresponding experimental or computational results. In the following such an extraction will be performed by using a similar approach.

Table 2
Values of E/R for CH_4/air flames at a pressure of 1 atm or 1 bar.

Author	Investigated range of ϕ	Pressure	E/R (K)
Present	0.512–0.601	1 atm	53,568
Göttgens et al. [38]	0.4–1.0	1 bar	23,873
Gu et al. [10]	0.8–1.2	1 bar	12,530

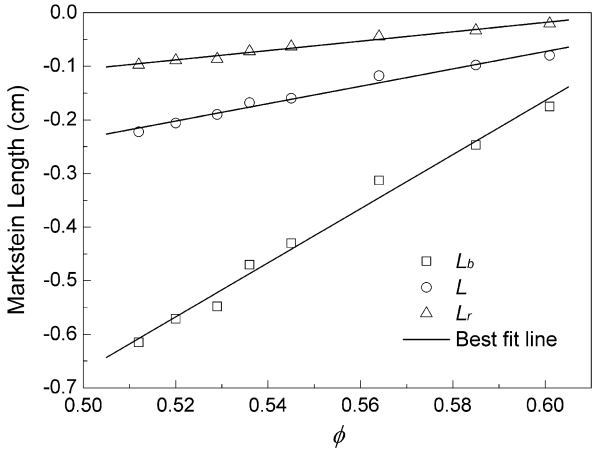

Fig. 9. Variations of Markstein lengths with equivalence ratio.

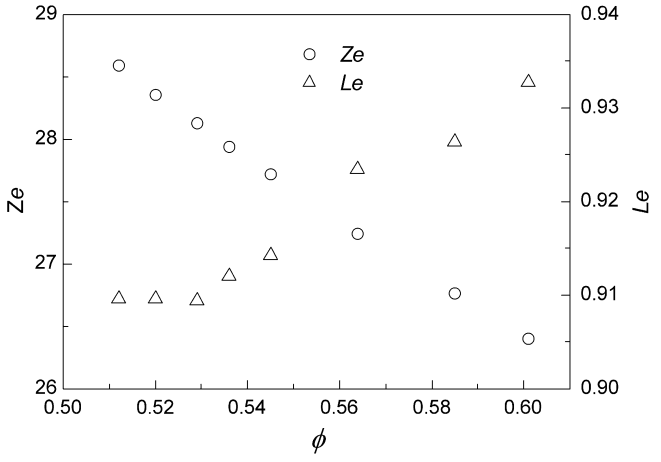

Fig. 10. Zeldovich number and extracted Lewis number as a function of equivalence ratio.

Theoretical analyses of stretched flames [29,47] showed that, for weakly stretched flames, u_L varies with α according to

$$u_L = u_{L0} + \frac{Ze}{2}\left(\frac{1}{Le} - 1\right)\delta_0\alpha \tag{15}$$

where δ_0 is a characteristic thickness of the one-dimensional unstretched flame. Thus, for a given mixture, u_L is expected to vary linearly with α. Reference to the expression of $u_L = u_{L0} - L\alpha$, given by Eq. (9), shows that

$$L = \frac{Ze}{2}\left(1 - \frac{1}{Le}\right)\delta_0 \tag{16}$$

In the present work δ_0 was independently calculated based on the definition $\delta_0 = (T_b - T_u)/(\mathrm{d}T/\mathrm{d}x)_{max}$ (x is the coordinate normal to the flame front), whereas L and Ze were found from experimental measurements. The extracted Lewis numbers from Eq. (16) are plotted as a function of ϕ in Fig. 10. It is noted that they are in reasonable range of anticipated values for very lean CH_4/air mixtures, slightly less than unity. Specifically, the evaluation of *Le* on basis of the diffusivity of the deficient species (CH_4) with the abundant species (N_2) yielded a constant of 0.93 for $\phi = 0.512$–0.601, while the corresponding extracted *Le* varies approximately from 0.91 to 0.93. Fig. 10 also shows that *Le* keeps nearly unchanged for sufficiently lean mixtures but steadily increases from $\phi \approx 0.53$ as ϕ increases. This indicates that an essentially constant *Le* based on the mass diffusivity of CH_4 may be acceptable only for the near-limit flames.

5. Conclusions

A microgravity environment has been utilized to accurately measure the near-limit properties of laminar premixed methane/air flames, with the burning velocity and effects of flame stretch in particular. Measurements were based on motion picture schlieren photographs of outwardly propagating spherical flames. Very lean CH_4/air mixtures were studied at a constant temperature of 298 ± 2 K and atmospheric pressure (1 atm) with equivalence ratios of 0.512–0.601. The major conclusions of the present study are as follows:

1. Effects of flame stretch were substantial under the investigated conditions, resulting in variations up to 2.1–3.9 times in the stretched burning velocity and corresponding variations of the flame speed in a range of 1.6–3.1 times. For all measured mixtures increasing stretch had a favorable effect on the increase of flame speed and burning velocity, yielding negative Markstein lengths. Absolute values of Markstein lengths were found to decrease linearly with equivalence ratio.
2. Present measurements of unstretched laminar burning velocities are quite close to previous microgravity results of Ronney and Wachman [20] at all measured equivalence ratios. Other previous measurements using a variety of experimental techniques at 1-g, however, gave higher values in general. The present data were compared also with numerical predictions based on three different chemical reaction mechanisms. The agreement is not satisfactory at all, with predictions invariably producing considerably higher values, although the prediction of the GRI-Mech kinetics seems better than those of other mechanisms. Discrepancies among various predictions and experiments clearly merit additional study.
3. Laminar burning velocity at the flammability limit is extremely small and was determined to be 1.2 cm/s.
4. The overall activation energy was determined from the variation of the laminar burning flux with flame temperature. Its value is much higher than those obtained previously by other workers, but was suggested to be more pertinent to near-limit flame propagation. The Zeldovich number calculated from the activation energy decreases with equivalence ratio.
5. Present results have been correlated to extract the flame Lewis number for use in the analytical expression describing the stretched flame response. In the range of $\phi > 0.53$ the extracted values were shown to increase steadily with equivalence ratio, highlighting the special significance of the extraction approach for off-limit flames.

Acknowledgments

The authors acknowledge the support of the European Commission under the Marie Curie Fellowships for Transfer of Knowledge contract MTKD-CT-2004-509847. The first author (S.F. Wang) was sponsored by the same grant during his stay in Poland. Partial support from the National Natural Science Foundation of China Grant 50576041 for this work is also appreciated.

References

[1] G.E. Andrews, D. Bradley, Combust. Flame 19 (1972) 275–288.
[2] C.J. Rallis, A.M. Garforth, Prog. Energy Combust. Sci. 6 (1980) 303–329.
[3] C.M. Vagelopoulos, F.N. Egolfopoulos, Proc. Combust. Inst. 27 (1998) 513–519.
[4] C.M. Vagelopoulos, F.N. Egolfopoulos, C. K Law, Proc. Combust. Inst. 25 (1994) 1341–1347.
[5] F.N. Egolfopoulos, D.L. Zhu, C.K. Law, Proc. Combust. Inst. 23 (1990) 471–478.
[6] A.F. Ibarreta, C.J. Sung, T. Hirasawa, H. Wang, Combust. Flame 140 (2005) 93–102.
[7] I. Yamaoka, H. Tsuji, Proc. Combust. Inst. 20 (1984) 1883–1892.
[8] K.T. Aung, L.-K. Tseng, M.A. Ismail, G.M. Faeth, Combust. Flame 102 (1995) 526–530.
[9] M.I. Hassan, K.T. Aung, G.M. Faeth, Combust. Flame 115 (1998) 539–550.
[10] X.J. Gu, M.Z. Haq, M. Lawes, R. Woolley, Combust. Flame 121 (2000) 41–58.
[11] D. Bradley, R.A. Hicks, M. Lawes, C.G.W. Sheppard, R. Woolley, Combust. Flame 115 (1998) 126–144.
[12] L. Qiao, Y. Gu, W.J.A. Dahm, E.S. Oran, G.M. Faeth, Proc. Combust. Inst. 31 (2007) 2701–2709.
[13] A. van Maaren, D.S. Thung, L.P.H. de Goey, Combust. Sci. Technol. 96 (1994) 327–344.
[14] K.J. Bosschaart, L.P.H. de Goey, Combust. Flame 136 (2004) 261–269.
[15] C.K. Law, G.M. Faeth, Prog. Energy Combust. Sci. 20 (1994) 65–113.
[16] P.D. Ronney, Proc. Combust. Inst. 27 (1998) 2485–2506.
[17] P.D. Ronney, in: H.D. Ross (Ed.), Microgravity Combustion: Fire in Free Fall, Academic Press, San Diego, 2001, pp. 35–82.
[18] R.A. Strehlow, D.L. Reuss, in: T.H. Cochran (Ed.), Combustion Experiments in a Zero Gravity Laboratory, Progress in Aeronautics and Astronautics, vol. 73, AIAA, New York, 1981, pp. 61–89.
[19] R.A. Strehlow, K.A. Noe, B.L. Wherley, Proc. Combust. Inst. 21 (1986) 1899–1908.
[20] P.D. Ronney, H.Y. Wachman, Combust. Flame 62 (1985) 107–119.
[21] P.D. Ronney, Combust. Flame 62 (1985) 121–133.
[22] H. Zhang, F.N. Egolfopoulos, Proc. Combust. Inst. 28 (2000) 1875–1882.
[23] K. Maruta, M. Yoshida, Y. Ju, T. Niioka, Proc. Combust. Inst. 26 (1996) 1283–1289.
[24] J. Jarosinski, J. Podfilipski, A. Gorczakowski, Combust. Sci. Technol. 174 (2002) 21–48.
[25] J. Jarosinski, J. Podfilipski, Y.K. Pu, Combust. Sci. Technol. 158 (2000) 183–194.
[26] D. Bradley, P.H. Gaskell, X.J. Gu, Combust. Flame 104 (1996) 176–198.
[27] P. Clavin, Prog. Energy Combust. Sci. 11 (1985) 1–59.
[28] G.H. Markstein, Non-steady Flame Propagation, Pergamon, New York, 1964.
[29] C.K. Law, C.J. Sung, Prog. Energy Combust. Sci. 26 (2000) 459–505.
[30] R.J. Kee, J.F. Grcar, M.D. Smooke, J.A. Miller, A Fortran Programming Tool for Modeling Steady Laminar One-dimensional Premixed Flames, Technical Report SAND85-8240, Sandia National Laboratories, 1985.
[31] G.P. Smith, D.M. Golden, M. Frenklach, N.W. Moriarty, B. Eiteneer, M. Goldenberg, C.T. Bowman, R.K. Hanson, S. Song, W.C. Gardiner Jr., V.V. Lissianski, Z. Qin. <http://www.me.berkeley.edu/gri-mech/>.
[32] C.R. Wilke, J. Chem. Phys. 18 (1950) 517–519.
[33] R.B. Bird, W.E. Stewart, E.N. Lightfoot, Transport Phenomena, John Wiley and Sons, New York, 1960.
[34] S. Mathur, P.K. Tondon, S.C. Saxena, Mol. Phys. 12 (1967) 569–579.
[35] F.A. Williams, Combustion Theory, second ed., Benjamin-Cummings, Menlo Park, CA, 1985.
[36] R.A. Strehlow, L.D. Savage, Combust. Flame 31 (1978) 209–211.
[37] G.E. Andrews, D. Bradley, Combust. Flame 18 (1972) 133–153.
[38] J. Göttgens, F. Mauss, N. Peters, Proc. Combust. Inst. 24 (1992) 129–135.
[39] F. Mauss, N. Peters, in: N. Peters, B. Rogg (Eds.), Reduced Kinetic Mechanisms for Applications in Combustion Systems, Lect. Notes Phys. 15 (1993) 58–75.

[40] K.N. Lakshmisha, P.J. Paul, N.K.S. Rajan, G. Goyal, H.S. Mukunda, Proc. Combust. Inst. 22 (1988) 1573–1580.
[41] V. Giovangigli, M. Smooke, Combust. Sci. Technol. 87 (1992) 241–256.
[42] K.N. Lakshmisha, P.J. Paul, H.S. Mukunda, Proc. Combust. Inst. 23 (1990) 433–440.
[43] N. Peters, F.A. Williams, Combust. Flame 68 (1987) 185–207.
[44] D. Bradley, in: J. Wearing (Ed.), Internal Combustion Engineering: Science and Technology, Elsevier Applied Science, London, 1990, p. 287.
[45] C.J. Sun, C.J. Sung, D.L. Zhu, C.K. Law, Proc. Combust. Inst. 26 (1996) 1111–1120.
[46] C.J. Sun, C.J. Sung, L. He, C.K. Law, Combust. Flame 118 (1999) 108–128.
[47] S.H. Chung, C.K. Law, Combust. Flame 72 (1988) 325–336.